THE ASTROPHYSICAL JOURNAL, 263:615–623, 1982 December 15

VLBI OBSERVATIONS OF THE NUCLEUS AND JET OF M87

M. J. REID AND J. H. M. M. SCHMITT
Harvard-Smithsonian Center for Astrophysics
F. N. OWEN
National Radio Astronomy Observatory[1]
R. S. BOOTH AND P. N. WILKINSON
Nuffield Radio Astronomy Observatory
D. B. SHAFFER
Phoenix Corporation
K. J. JOHNSTON
E. O. Hulburt Center for Space Research, US Naval Research Laboratory
AND
P. E. HARDEE
University of Alabama
Received 1982 March 22; accepted 1982 June 14

ABSTRACT

We mapped the nucleus and jet of M87 with an eight-station very long baseline interferometric (VLBI) array at 18 cm wavelength with high dynamic range. The nucleus of M87 consists of a "core-jet" structure with a peak brightness temperature greater than 10^{10} K. Emission extends for more than 50 milli-arcsec (mas) with a brightness temperature exceeding 10^8 K along a position angle of 288°. This position angle precisely matches that of the 20″ radio/optical/X-ray jet. The nucleus also contains significant structure of lower brightness ($S \approx 0.5$ Jy and extent greater than 0″.1) at approximately the same position angle. No "counterjet" is seen. If relativistic beaming is invoked to enhance the jet and diminish the counterjet, then the jet must be aligned within about 60° to our line of sight, and its flow velocity must exceed about 60% of the speed of light. The nuclear structure does not bend measurably, but our data suggest that it might wiggle slightly.

No compact structures were detected in the knots of the 20″ jet which extends from near the nucleus to the northwest radio lobe. Any structure less than 4 mas in size must be weaker than 25 mJy, and any structure less than 0″.1 must be weaker than 0.2 Jy. The innermost knot (knot D) has a Gaussian FWHM between 0″.1 and 0″.3.

Subject headings: galaxies: individual — galaxies: nuclei — galaxies: structure — interferometry

I. INTRODUCTION

M87 (3C 274, Virgo A, NGC 4486) is an E0 galaxy with a redshift of 0.004. Its radio emission consists of two extended lobes separated by about 50″ which are embedded in a 10′ halo. At the center of the source, coincident with the nucleus of the galaxy, is a compact component. A bright jet extends about 20″ toward the northwestern lobe. This jet contains knots, some of which have been detected in X-rays (Schreier, Feigelson, and Gorenstein 1982), at optical wavelengths (e.g., de Vaucouleurs and Nieto 1979), and at radio frequencies (e.g., Wilkinson 1974; Turland 1975; Laing 1980; Owen, Hardee, and Bignell 1980; Charlesworth and Spencer 1982).

[1]The National Radio Astronomy Observatory is operated by Associated Universities, Inc., under contract to the National Science Foundation.

The Very Large Array (VLA) maps of Owen, Hardee, and Bignell (1980) show that the innermost knot of the jet is smaller than 0″.3, and the strongest knot is about 1″ in diameter. In the optical band (de Vaucouleurs and Nieto 1979), as well as in the radio band, the knots increase in size with distance from the nucleus. The VLA maps also show abrupt changes in polarization near the knot boundaries. Owen, Hardee, and Bignell (1980) suggest that this structure could arise if a shock front is present at the outer edge of a knot. In this case, with sufficient sensitivity and resolution, it may be possible to detect small-scale structure elongated perpendicular to the jet.

Very little is known about the compact nuclear component. There appears to be structure on all size scales from less than 0″.001 to greater than 0″.1 (e.g., Donaldson, Miley, and Palmer 1971; Kellermann *et al.*

1973; Shaffer and Schilizzi 1975). The very long baseline interferometric (VLBI) map at 13 cm wavelength by Cotton, Shapiro, and Wittels (1981) shows that the nuclear structure extends toward the northwest.

In order to study both the nucleus and the jet of M87, we conducted an eight-station intercontinental VLBI experiment. At the observing wavelength of 18 cm, the array was sensitive to structures from 0".004 to 0".1. We made a hybrid map of the nucleus of M87 with high dynamic range and searched for compact structures within the knots of the jet.

II. OBSERVATIONS AND DATA ANALYSIS

M87 was observed on 1980 February 12 at 1666.52 MHz in right-circular polarization. The station names and details of the observing equipment are given in Table 1. All data were collected with Mk II VLBI terminals (Clark 1973) and were cross-correlated on the NRAO three-station processor.

These observations were the first to use the VLA as an element of a VLBI array. Only one antenna of the VLA was used to avoid resolving the 20" radio jet of M87 (with the VLA itself). Unfortunately, the local oscillator system was configured in such a manner that its long-term stability was limited by a crystal oscillator, rather than the rubidium vapor frequency standard which had been moved from the HRAS station to the VLA for this experiment. This resulted in a short coherence time of about 60 s for interferometer pairs involving the VLA. In order to increase the coherent integration time, we phase referenced all data on these interferometer pairs with phases determined for M87 from the OVRO–VLA baseline. This baseline was sufficiently sensitive to detect fringes on M87 with less than 60 s integration. The phase-referencing procedure extends the coherent integration time for interferometer pairs involving the VLA. Since a single phase versus time function was subtracted from all data involving the VLA station, this procedure does not affect the closure phases (i.e., phases summed around an interferometer triangle) used in the hybrid-mapping scheme.

The interferometer amplitudes were first calibrated using radiometry data from each telescope. We adopted a value of 2.5 for the overall losses (b-factor; see Cohen *et al.* 1975) in the Mk II digital recording and processing system. The calibrated data were then analyzed with the Caltech hybrid-mapping procedure (Readhead and Wilkinson 1978). This procedure calculates individual interferometer phases from the observed closure phases and a source model. The data are then Fourier inverted and "CLEANed" to produce a map. The resultant map is used as the basis of a new source model, and the procedure is repeated until the maps appear to converge. Extensive tests with artificial data have shown that this procedure yields images which are faithful representations of the source structure, independent of the initially assumed source model, provided that sufficient data exist to constrain the process (Readhead and Wilkinson 1978). We expect that this condition should be well satisfied for our data. We chose an initial point-source model for M87 in order to avoid any possible bias in source position angle.

The dynamic range (i.e., the peak brightness to the weakest believable feature) of the hybrid map, produced in the standard manner, was about 20 to 1. The dynamic range was primarily limited by systematic errors in the calibration, caused by greater than 10% uncertainties in the radiometry results from some stations. In order to improve the calibration, we performed an amplitude "self-calibration" procedure similar, in principle, to those described by Readhead *et al.* (1980), Rogers (1980), and Schwab (1980) for interferometer data. A constant scaling parameter for each telescope (except one, NRAO) was varied so as to minimize the sum of the squares of the deviations of the observed interferometer amplitudes from those predicted by the model. We feel that the

TABLE 1

VERY LONG BASELINE INTERFEROMETRIC ARRAY PARAMETERS

Observatory	Location	Diam. (m)	Frequency Standard	Receiver Type	$(2kT_{sys}/A_{eff})$[a] (Jy)
Nuffield Radio Lab. (JDRL)	Jodrell Bank, UK	76	Rubidium	Paramp	480
Haystack Obs. (HAYS)	Westford, MA	37	H maser	Paramp	2190
Naval Research Lab. (NRL)	Md. Point, MD	26	H maser	Paramp	1970
National Radio Astronomy Obs. (NRAO)	Green Bank, WV	43	H maser	Cooled paramp	350
North Liberty Radio Obs. (NLRO)	Iowa City, IA	18	Rubidium	Cooled FET	7100
Harvard Radio Astronomy Station (HRAS)	Ft. Davis, TX	26	H maser	Paramp	1020
National Radio Astronomy Obs. (VLA)	Socorro, NM	26	Crystal	Cooled FET	750
Owens Valley Radio Obs. (OVRO)	Big Pine, CA	40	H maser	Paramp	740

[a] This quantity is the system temperature expressed in Jy; it is inversely proportional to the sensitivity of the station; k is Boltzmann's constant, T_{sys} is the system temperature on M87, and A_{eff} is the effective collecting area of the telescope.

final calibration, corrected with these scaling parameters, has a precision of about 3% and is limited primarily by small variations in system temperature that are unaccounted for. The uncertainty in our flux density scale is about 5% (which does not affect the dynamic range of the map). It was determined using radiometry data at the NRAO 43 m telescope and assumes a flux density of 167 Jy for the partially resolved M87 source (cf. Baars 1977). The final dynamic range of the map is better than 50 to 1.

The interferometer (u, v)-coverage for M87 in this experiment is shown in Figure 1. The main lobe of the "dirty beam," i.e., the point-source response for the (u, v)-coverage, has a full width at half-maximum (FWHM) of 18 by 4 milli-arcsec (mas) elongated at a position angle of $-11°$ east of north. Since there is no complex structure perpendicular to the jet, we used a circular Gaussian restoring beam of 8 mas, which is the FWHM of the dirty beam along the jet position angle of 288°.

It is difficult to map the knots in M87 with a VLBI array because of (1) dynamic range problems due to the proximity of the high-brightness nucleus, (2) the intrinsic weakness of any compact components in the knots, and (3) the large number of picture elements between the nucleus and the knots (e.g., 10,000 for knot A). Even if one could afford the computational effort to construct a map large enough to include the nucleus and the knots, one could not use the usual hybrid-mapping technique, which requires detectable fringes on all baselines for each integration period. The allowable integration time is limited by the field of view of the map because of rapid variations of interferometer phase on long baselines for emission far from the map center. A field of view of 10″ would limit the integration on the longer baselines to less than 10 s, while detection of the nucleus on "weak" baselines required integration times of greater than 300 s.

In order to map the knots, the data were phase referenced to the nucleus. This procedure involved fitting fringes to the data for all baselines involving a reference station (i.e., a reference station was arbitrarily chosen to have zero phase) in order to construct tables of phase versus time for each station. These tables were generated using 600 s integrations on M87 and were corrected for the effects of the nuclear structure on the fringe phases. Finally, the complex fringe visibilities on all baselines were multiplied by $\exp[-i2\pi(\phi_b - \phi_a)]$, where ϕ_x is the phase of station x from the phase tables. Phase referencing removes the effects of local oscillator variations, baseline and source coordinate uncertainties, and atmospheric and ionospheric irregularities from the data. Next, the contribution of the nucleus was subtracted from the complex visibility data. Finally, the interferometer phase center was shifted to the location of a knot, and a map was made by Fourier inverting the data. As a test, a map at the location of the nucleus was made from these data. This map had a residual flux density level of only about 0.1 Jy. At this level, dynamic range problems for mapping knots greater than 1″ from the nucleus are insignificant.

III. RESULTS AND DISCUSSION

a) *Morphology*

The map (Fig. 2) clearly shows that the nucleus of M87 contains a one-sided jet. This morphology is similar to that observed in many compact extragalactic sources. The position angle of the jet is 288° (±3°) (east of north), which matches that of the 20″ radio/optical/X-ray jet. Compared to the 20″ jet, no bending through an angle greater than about 5° is observed. Readhead *et al.* (1978) point out that jets which bend on milli-arcsec scales are found in C-type sources (i.e., sources whose compact, central component is dominant), whereas straight jet structures are found in S-type sources (i.e., sources whose symmetric, extended lobes are dominant). Since the radio morphology of M87 is best described as S-type, the absence of a bent nuclear jet supports this correlation.

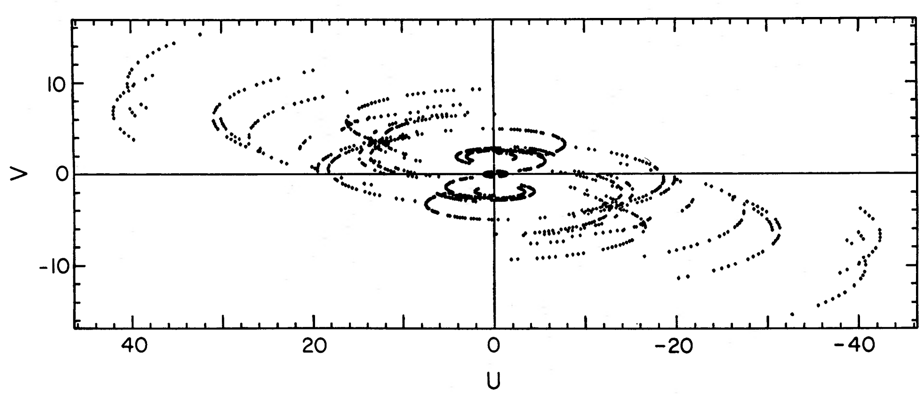

FIG. 1.—(u, v)-coverage from the eight-station intercontinental VLBI experiment on M87 at 18 cm wavelength. Units are 10^6 wavelengths. East is to the left and north is to the top.

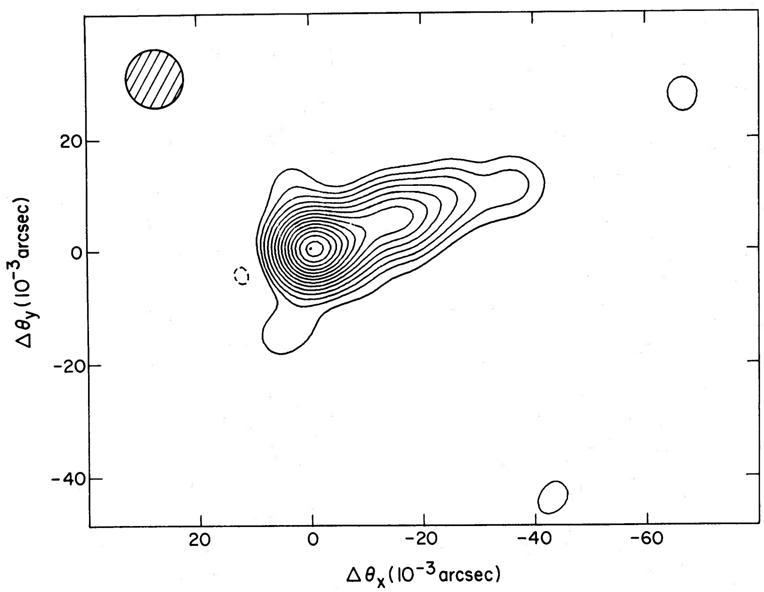

FIG. 2.—Nucleus of M87 at 18 cm wavelength. Contours are −1.5, 1.5, 3, 5, 8, 12, 17, 23, 30, 38, 47, 57, 68, 80, and 93% of the peak brightness of 9.0×10^9 K. Restoring beam (*upper left*) is an 8 mas FWHM circular Gaussian. East is to the left and north is to the top.

In Figure 3 we plot the intensity of the nucleus versus distance along the jet (along a position angle of 288°). The brightest component is well modeled by an 8.9 mas circular Gaussian component (FWHM), which has been subtracted and plotted with a dashed line. Since the restoring beam was 8.0 mas, this component corresponds to a 4 mas source with a brightness temperature of 4.5×10^{10} K. Emission is detected up to about 50 mas from the nucleus, where the brightness temperature drops below our threshold of 10^8 K. The jet appears unresolved perpendicular to its extent. Specifically, the sizes (FWHM) for a Gaussian model are approximately less than 4 mas for the brightest component, less than 5 mas for components 15 mas down the jet, and less than 7 mas for components 40 mas down the jet.

In Figure 4 we plot the observed amplitudes and closure phases and those derived from the hybrid-mapping procedure. The map adequately reproduces the observed fringe amplitudes and closure phases for all but the shortest projected interferometer spacings. On several short baselines, when the fringe spacing becomes perpendicular to the jet, a significant increase in fringe amplitude is observed (e.g., at 21^h GST on NRAO–HAYS and 20^h GST on NRL–HAYS). This indicates that the nucleus contains a very elongated component ($> 0''.1$) which extends along the same position angle as the jet. This component is fully resolved at the vast majority of our (u, v)-points, and we could not map it. The integrated flux density of this resolved component is roughly 0.5 Jy. Although we cannot precisely locate its position, it must be within about $1''$ of the brightest spot in the nucleus. Otherwise, the fringe rate of the component would differ from that of the nucleus sufficiently to be degraded with our 600 s integrations. We are unable to determine whether this low-brightness component is the "missing counterjet," a continuation of the emission seen in the map at lower brightness, or a nuclear halo.

We wish to point out the possibility that the nuclear jet "wiggles" slightly. The data from our longer baselines are modeled slightly better by a jet that has a peak-to-peak oscillation on the order of 3 mas (perpendicular to its extent) and a characteristic wavelength of roughly 10–30 mas than by a straight jet. Although this structure exists in the CLEAN components, it is partially masked by the 8 mas restoring beam, which smooths over a large fraction of an oscillation period. We have conducted extensive checks of our data analysis programs and are confident that such wiggles are not a computational artifact.

It is interesting to note that structures which appear to wiggle can be found in published maps of other compact extragalactic sources, such as 3C 147 (Simon *et al.* 1980), 3C 286 (Wilkinson and Readhead 1979), and 3C 380 (Readhead and Wilkinson 1980). Models which might explain a wiggling jet include a precessing central source, such as in SS 433 (cf. Hjellming and Johnston 1981) and 3C 129 (Icke 1981), and instabilities in the jet flow (cf. Hardee 1982; Ferrari *et al.* 1982). However, since further observations are needed to confirm the reality of the wiggles in the nucleus of M87, as well as in other sources, a detailed discussion of these possibilities seems premature.

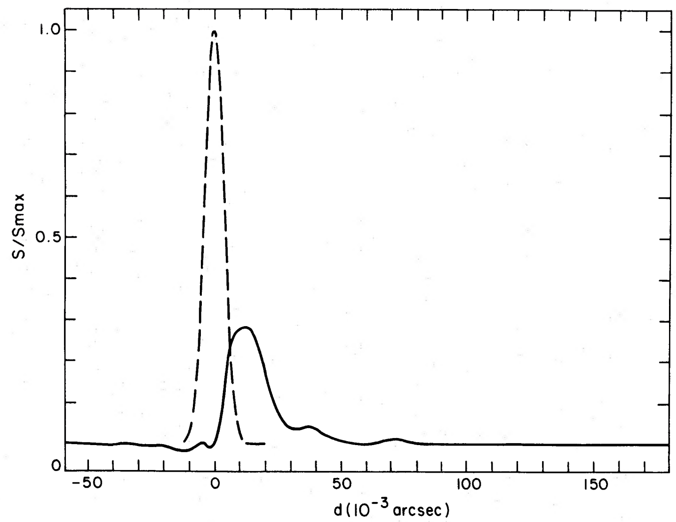

FIG. 3.—Intensity of the map shown in Fig. 2 vs. position along 288° position angle. A Gaussian component with FWHM of 8.9 mas (*dashed line*) was subtracted from plot.

b) *Counterjet*

The existence of the southeast lobe in M87 clearly indicates the existence (at some time at least) of a counterjet to transport energy out from the central source. However, even with the high dynamic range of our map we see no signs of a nuclear counterjet. The low brightness of postulated counterjets in compact extragalactic radio sources is usually explained in the context of special relativity. A luminous object moving with velocity v at an angle θ relative to the observer's line of sight will be observed to have a spectral intensity $I_{ob}(\nu_{ob})$, given by

$$I_{ob}(\nu_{ob}) = I(\nu)D^3, \quad (1)$$

where I is the spectral intensity (i.e., units of ergs s^{-1} cm^{-2} Hz^{-1} sr^{-1}) in a reference frame at rest with the object, D is the relativistic Doppler factor given by

$$D = \frac{[1-(v/c)^2]^{1/2}}{1-(v/c)\cos\theta}, \quad (2)$$

and c is the speed of light. Since $\nu_{ob} = D\nu$, equation (1) can be rewritten as

$$I_{ob}(\nu_{ob}) = I(\nu_{ob})D^{3+\alpha}, \quad (3)$$

where α is the spectral index of the source (i.e., $I \propto \nu^{-\alpha}$). If the jet is continually (or episodically) supplied with components at its base and the emission ceases after a given time (or distance down the jet), then differences between source lifetimes in the two reference frames remove one Doppler factor (see Scheuer and Readhead 1979 and references therein), and equation (3) becomes

$$I_{ob}(\nu_{ob}) = I(\nu_{ob})D^{2+\alpha}. \quad (4)$$

Assuming that the absence of a detectable counterjet is due to the effects just discussed, one can place limits on the flow velocity (v) of the jet and the angle (θ) between the jet and our line of sight. Defining R as the ratio of the observed intensity of the jet and counterjet and assuming $\alpha = 0.5$ (cf. Readhead and Wilkinson 1980), one obtains

$$R = \left[\frac{1+\beta\cos\theta}{1-\beta\cos\theta}\right]^{2.5}, \quad (5)$$

where $\beta = v/c$. Solving for $\beta\cos\theta$, we find that

$$\beta\cos\theta = \frac{R^{0.4}-1}{R^{0.4}+1}. \quad (6)$$

Our observations of M87 require an intensity ratio of nearly 100 to 1 between the brightest component in the map and the upper limit to the intensity level at the location of a possible counterjet. However, the brightest component could be the central energy source, and its intensity might not be enhanced by beaming. Hence, for the following discussion we will adopt a conservative intensity ratio between jet and counterjet of 28 to 1, appropriate for the component(s) 15 mas along the jet. $R = 28$ requires $\beta\cos\theta > 0.6$, and, since both β and $\cos\theta$ are bounded by 1, this requires $\beta > 0.6$ and $\cos\theta > 0.6$. Therefore, if the absence of a detectable counterjet

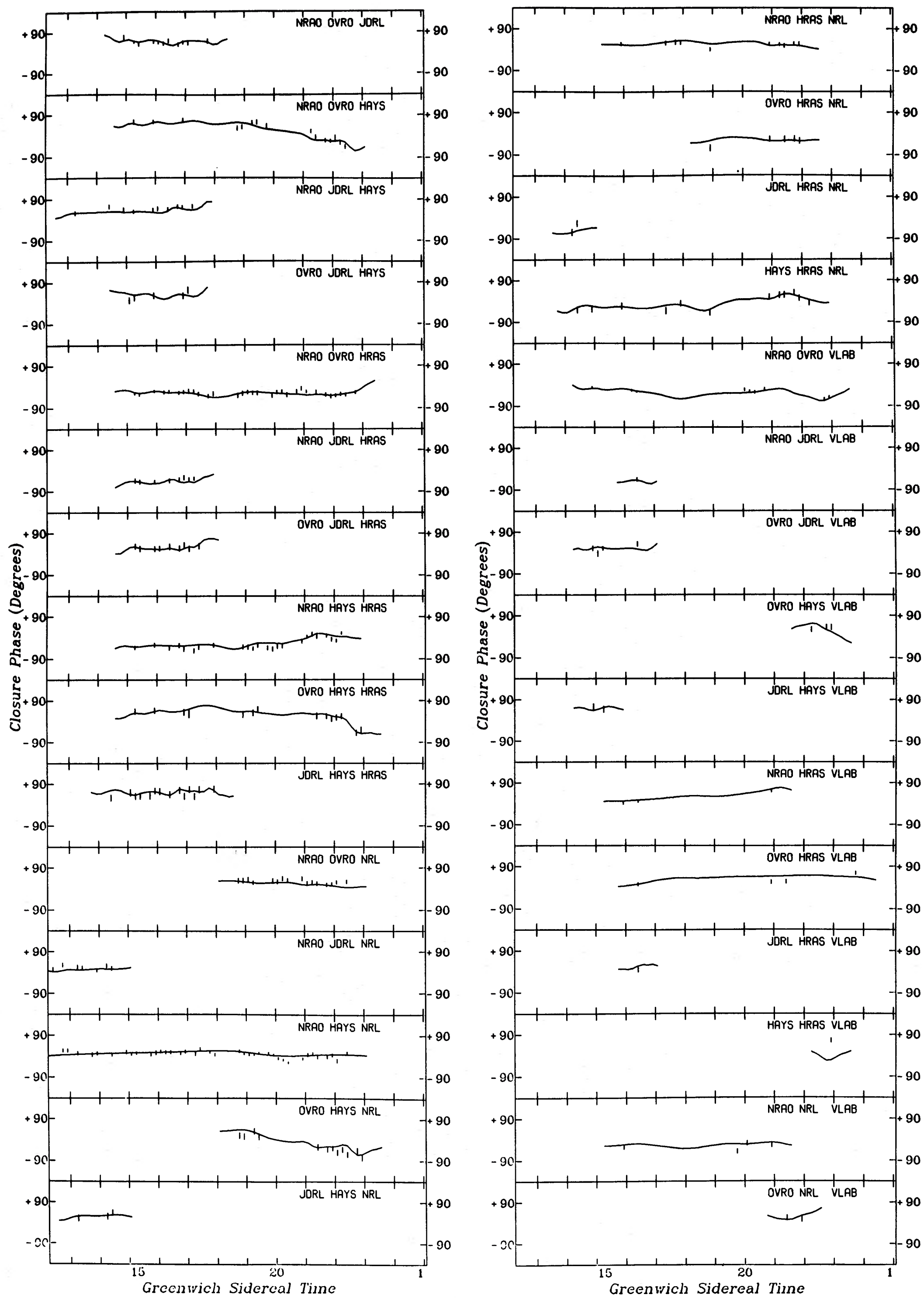

FIG. 4.—Observed interferometer fringe amplitudes and closure phases (*vertical bars*) vs. Greenwich Sidereal Time. Values predicted by a model derived from the map (Fig. 2) are shown with solid line. Lengths of the bars indicate ±1 sigma uncertainties which for the amplitudes include an allowance of 3% for systematic scaling errors among different telescopes.

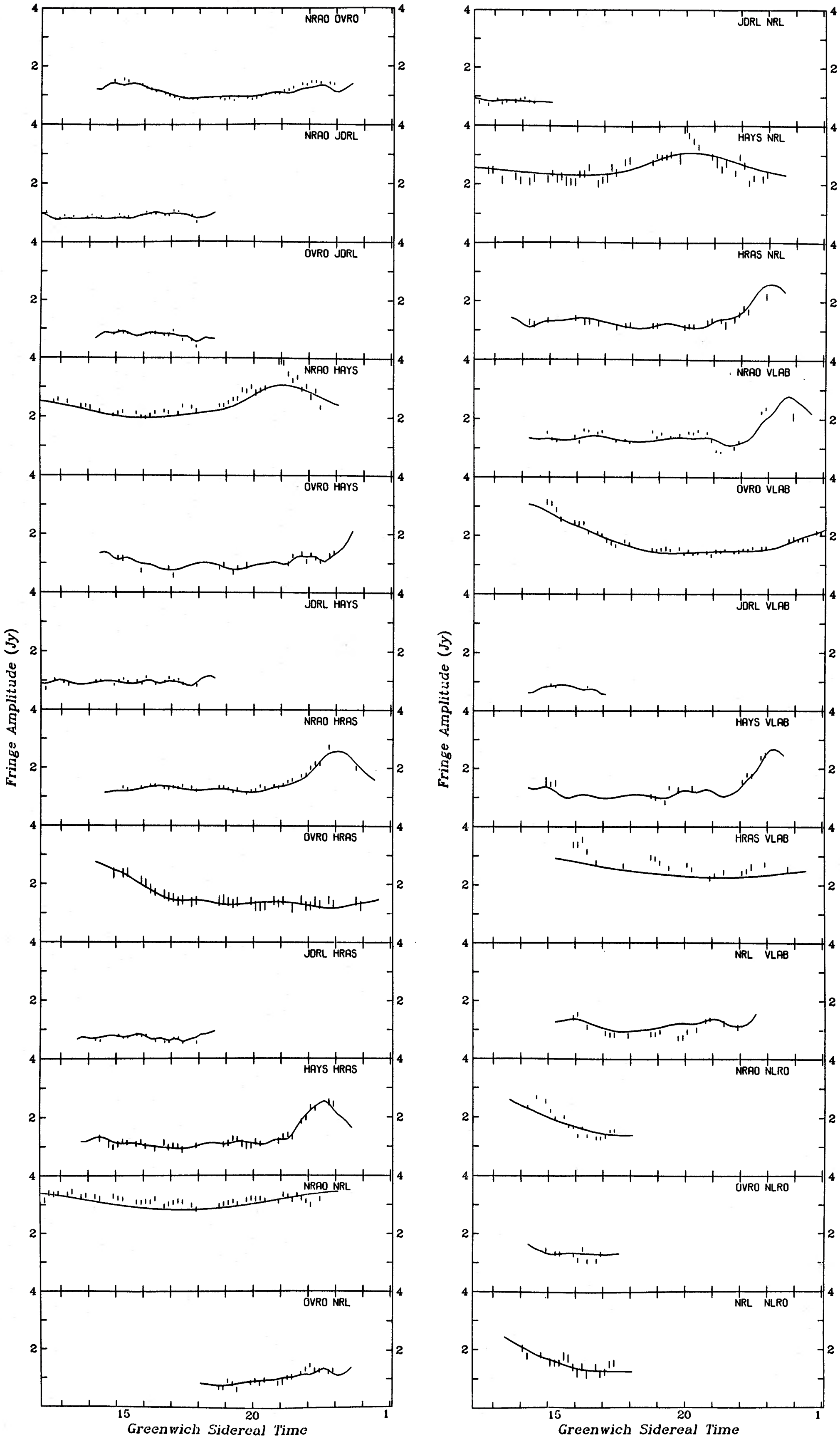

FIG. 4.—*Continued*

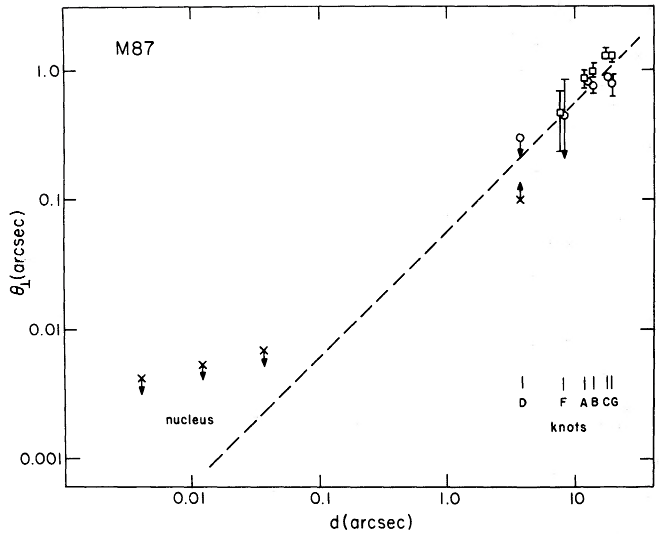

FIG. 5.—Angular size ($\theta_\perp$) perpendicular to the jet for the nucleus and some of the knots as a function of distance (d) along the jet of M87. Sizes are full width at half-maximum (FWHM) for a Gaussian brightness distribution and are from the 18 cm VLBI results of this paper (*crosses*), the 6 and 2 cm VLA results of Owen, Hardee, and Bignell (1980) (*circles*), and the optical results of de Vaucouleurs and Nieto (1979) (*squares*).

is due to relativistic effects, then the jet flow velocity must exceed $0.6c$, and the angle between the jet and our line of sight must be less than about 60°.

There are, of course, other possible explanations for the absence of an observed counterjet, such as that jets are intrinsically one-sided and may alternate sides from time to time (Rudnick 1982). One crucial observation would be to detect proper motion of components within the jet. If components move with the jet flow, then their observed velocity on the plane of the sky $v_{\perp_{\rm ob}}$ should be given by

$$v_{\perp_{\rm ob}} = \frac{v_\perp}{1-\beta\cos\theta}, \qquad (7)$$

where $v_\perp = v\sin\theta$. For $\beta > 0.6$ and $\beta\cos\theta > 0.6$, $v > 1.5c(\sin\theta)$. At a distance of $12/h$ Mpc ($H_0 = 100h$ km s^{-1} Mpc^{-1}) for M87 and for $\theta > 5°$, this implies a proper motion of greater than $0.8h$ mas yr^{-1}, which would be detectable with a second epoch map. However, for $\beta = 1$, the proper motion would be greater than $8h$ mas yr^{-1} for any $\theta < 60°$.

c) *Knots*

In addition to the nucleus of M87, we mapped portions of the jet encompassing knots D and A (in the notation of de Vaucouleurs and Nieto 1979), which are 3″.2 and 12″.6, respectively, from the nucleus. (Details of the mapping procedure are given in § II.) Motivation for seeking compact structures in the knots comes from recent theories and observations of radio jets. Compact structures in jets could be due to shocks, which may be produced within the jet (Rees 1978) or by interaction with the external medium (Blandford and Königl 1979). Some support for shocklike structure in the jet comes from the polarization observations of Owen, Hardee, and Bignell (1980), which show abrupt polarization changes at knot A. Using data from most of the US baselines, we were able to place an upper limit of 25 mJy for any compact (< 4 mas) component within 0″.5 of the centroid of each knot. Using only our shortest baselines we place an upper limit of 0.2 Jy for any component smaller than 0″.1 (FWHM) and within 2″ of each knot center. Thus, our observations indicate that the emission from the knots is fairly smooth on scales less than 0″.1.

Owen, Hardee, and Bignell (1980), using the VLA, have determined an upper limit of 0″.3 (FWHM) for the innermost knot (knot D). Combining the two limits we conclude that $0''.1 < \theta_{\rm D} < 0''.3$, where $\theta_{\rm D}$ is the FWHM of a circular Gaussian source model for knot D. This result assumes that the angular size of the knot is independent of frequency between 1.6 and 15 GHz (as would be expected from an optically thin source), and that the total flux density of knot D at 18 cm is greater than 0.2 Jy (Charlesworth and Spencer 1982 measure 1.0 ± 0.3 Jy for knot D using the Multi-Telescope Radio-Linked Interferometer [MTRLI] network).

The present observations extend the angular size versus distance relation for the knots in the M87 jet, first noted in the optical by de Vaucouleurs and Nieto (1979). In Figure 5 we plot the angular size perpendicular to the jet $\theta_\perp$ as a function of distance down the jet d, from the nucleus to the knots. The line drawn in Figure 5 is for $\theta_\perp = 0.06\ d$, after de Vaucouleurs and Nieto. The data which span three orders of magnitude in d are consistent with this line. A modest increase in angular resolution or dynamic range may resolve the nuclear structure perpendicular to the jet and fully characterize the expansion of the jet. Precise details of the jet expansion are not yet known, but the present observations suggest a nearly uniform expansion of the jet at a few percent of the jet flow speed. If material flows down the jet at greater than $0.6c$, then this expansion speed is greater than 5000 km s^{-1}.

IV. SUMMARY

The nucleus of M87 shows an asymmetric "core-jet" structure extending for more than 50 mas toward the well-known 20″ radio/optical/X-ray jet. Our data also show evidence of significant structure on a scale greater than 0″.1 in the nucleus. If relativistic beaming is invoked to explain the apparent absence of a symmetric counterjet in the nucleus, then a jet flow velocity greater than $0.6c$ is required.

The knots embedded in the 20″ jet contain no bright, compact structures, and the size of the innermost knot (knot D) is between 0″.1 and 0″.3.

We thank K. Kellermann for helpful comments, and the US VLBI network for making these observations possible.

REFERENCES

Baars, J. W. H. 1977, *Astr. Ap.*, **61**, 99.
Blandford, R. D., and Königl, A. 1979, *Ap. J.*, **232**, 34.
Charlesworth, M., and Spencer, R. E. 1982, preprint.
Clark, B. G. 1973, *Proc. IEEE*, **61**, 1242.
Cohen, M. H, *et al.* 1975, *Ap. J.*, **201**, 249.
Cotton, W. D., Shapiro, I. I., and Wittels, J. J. 1981, *Ap. J. (Letters)*, **244**, L57.
de Vaucouleurs, G., and Nieto, J.-L. 1979, *Ap. J.*, **231**, 364.
Donaldson, W., Miley, G. K., and Palmer, H. P. 1971, *M.N.R.A.S.*, **152**, 145.
Ferrari, A., Massaglia, S., Trussoni, E., and Zaninetti, L. 1982, in *IAU Symposium 97, Extragalactic Radio Sources*, ed. D. S. Heeschen and C. M. Wade (Dordrecht: Reidel), p. 229.
Hardee, P. E. 1982, *Ap. J.*, **257**, 509.
Hjellming, R. M., and Johnston, K. J. 1981, *Ap. J. (Letters)*, **246**, L141.
Icke, V. 1981, *Ap. J. (Letters)*, **246**, L65.
Kellermann, K. I., Clark, B. G., Cohen, M. H., Shaffer, D. B., Broderick, J. J., and Jauncey, D. L. 1973, *Ap. J. (Letters)*, **179**, L141.
Laing, R. A. 1980, *M.N.R.A.S.*, **193**, 427.
Owen, F. N., Hardee, P. E., and Bignell, R. C. 1980, *Ap. J. (Letters)*, **239**, L11.
Readhead, A. C. S., Cohen, M. H., Pearson, T. J., and Wilkinson, P. N. 1978, *Nature*, **276**, 768.
Readhead, A. C. S., Walker, R. C., Pearson, T. J., and Cohen, M. H., 1980, *Nature*, **285**, 137.
Readhead, A. C. S., and Wilkinson, P. N. 1978, *Ap. J.*, **223**, 25.
______. 1980, *Ap. J.*, **235**, 11.
Rees, M. J. 1978, *M.N.R.A.S.*, **184**, 61P.
Rogers, A. E. E. 1980, *S.P.I.E. Proc.*, **231**, 23.
Rudnick, L. 1982, in *IAU Symposium 97, Extragalactic Radio Sources*, ed. D. S. Heeschen and C. M. Wade (Dordrecht: Reidel), p. 47.
Scheuer, P. A. G., and Readhead, A. C. S. 1979, *Nature*, **277**, 182.
Schreier, E., Feigelson, E., and Gorenstein, P. 1982, in preparation.
Schwab, F. 1980, *S.P.I.E. Proc.*, **231**, 18.
Shaffer, D. B., and Schilizzi, R. T. 1975, *A.J.*, **80**, 753.
Simon, R. S., Readhead, A. C. S., Moffet, A. T., Wilkinson, P. N., and Anderson, B. 1980, *Ap. J.*, **236**, 707.
Turland, B. D. 1975, *M.N.R.A.S.*, **170**, 281.
Wilkinson, P. N. 1974, *Nature*, **252**, 661.
Wilkinson, P. N., and Readhead, A. C. S. 1979, *Ap. J.*, **232**, 365.

R. N. Booth and P. N. Wilkinson: Nuffield Radio Astronomy Laboratories, Jodrell Bank, Macclesfield, Cheshire, UK

P. E. Hardee: Dept. of Physics and Astronomy, University of Alabama, P.O. Box 1921, University, AL 35486

K. J. Johnston: Code 7130, E. O. Hulburt Center for Space Sciences, US Naval Research Laboratory, Washington, DC 20375

F. N. Owen: National Radio Astronomy Observatory, P.O. Box O, Socorro, NM 87801

M. J. Reid and J. H. M. M. Schmitt: Harvard-Smithsonian Center for Astrophysics, 60 Garden St., Cambridge, MA 02138

D. B. Shaffer: NASA/GSFC, Code 974, Greenbelt, MD 20771